ACS APPLIED POLYMER MATERIALS

pubs.acs.org/acsapm
Article

Self-Healing Activation by Conventional Resistive Heating through the Addition of Carbon Nanotubes in Epoxy Systems Based on Covalent Adaptable Networks

Javier Gómez-Sánchez, Xoan Xosé Fernández Sánchez-Romate,* Alberto Jiménez-Suárez, and Silvia G. Prolongo

Cite This: ACS Appl. Polym. Mater. 2024, 6, 1106−1115

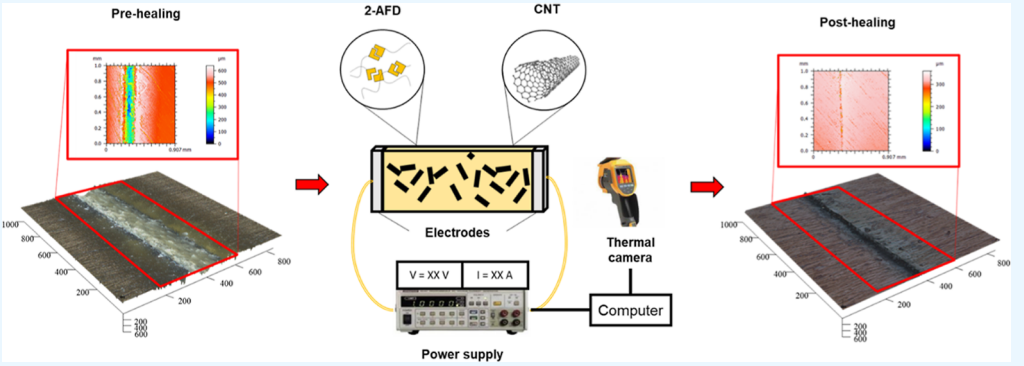

ABSTRACT: A study of the self-healing capabilities of 2-aminophenyl disulfide (AFD)/epoxy systems is carried out. It has been observed that an excess of AFD promotes an increase of both the storage modulus and the glass transition temperature (T_g) due to an increase of the cross-link density. Concerning the self-healing properties, every AFD/epoxy system shows very good healing efficiencies (above 90%) with no prevalent differences among the different stoichiometries. Furthermore, CNT addition induces an increase of the storage modulus when there is no excess of AFD, but no significant effect is observed on the T_g. In addition, the incorporation of these nanoparticles allows thermal activation by the Joule effect. The results of self-healing tests under convective and resistive heating show similar healing efficiencies (all above 94%). Here, the thermal activation by Joule's heating presents a lower power consumption and allows localized repair, which is very promising for this type of application.

KEYWORDS: *self-healing, Joule's effect, carbon nanotubes, AFD, epoxy matrix*

1. INTRODUCTION

Thermoset resins are commonly reinforced with fiber to obtain Fiber Reinforced Polymer (FRP) composites for high-performance structural applications due to their high cross-link density, low shrinkage, high rigidity, low creep, good wettability, and adhesion, as well as chemical resistance.[1] However, their excellent performance is usually degraded during their in-service life due to the brittle behavior of the epoxy resin, mainly caused by the high density of the benzene ring and the cross-linking density.[2] Consequently, in the presence of external factors such as mechanical loads, environmental conditions, etc., minor defects may be initiated. If these damages are not detected and solved, they may propagate among the volumes and lead to a catastrophic failure of the component.

The highly cross-linked structure of thermosets makes them difficult to repair, recycle, or reprocess. In the case of detecting critical damage affecting the overall structure performance, they require the application of patches that increase the weight of the component, decreasing the high strength-to-weight ratio inherent to the composite material, or even the full substitution of the component by a new one, resulting in a waste product. In both cases, reliability, safety, and maintenance costs suffer an unavoidable negative impact.

One possible solution could be the application of thermoplastics to composites since they can be reprocessed under a thermal stimulus. However, actual investigations are still far from reaching the high-performance properties of thermosets. This fact, together with the difficult manufacturing process involved in these materials, makes them only suitable for

Received: May 15, 2023
Revised: November 9, 2023
Accepted: November 10, 2023
Published: January 10, 2024

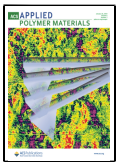

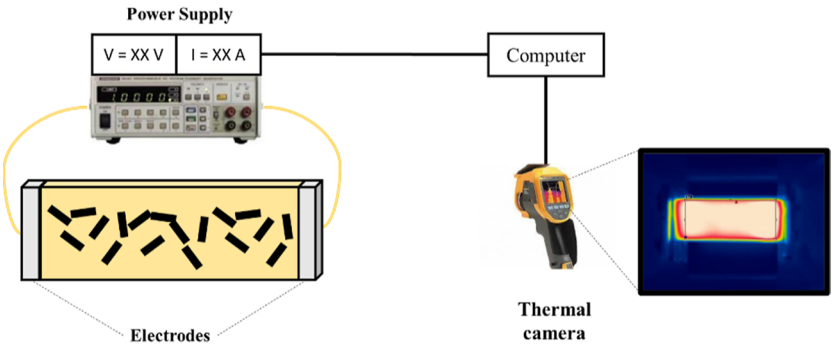

Figure 1. Schematics of Joule's heating tests.

secondary structures not supporting high loads.[3] For this reason, the incorporation of dynamic networks into thermoset polymers to provide them with self-healing functionality has attracted considerable attention due to its ability to repair damages and cracks, restoring the original properties of the material, and, thereby, extending its lifetime.[4,5]

From a literature review, self-healing mechanisms can be distinguished into three categories: physical interactions, supramolecular polymers, and chemical interactions.[6] Self-healing principles based on physical interactions rely on an excess of unreacted epoxy groups that behave as the healing agent in the formulation and react at a crack interface. These polymer blends can be miscible (dissolved in the resin[7,8]) or immiscible (capsules of an uncured self-healing agent released when broken under crack formation[9]). Supramolecular polymers are based on the recombination of noncovalent bonds to heal the damage,[10] such as hydrogen bridges,[11] ionic bonds,[12−14] and $\pi-\pi$ stacking.[15] The latter, based on chemical interactions, are related to the dynamic covalent bonds that become reversible when subjected to an external stimulus. Following this approach, many groups have achieved self-healing properties on thermosets by using dynamic exchange reactions.[16]

Disulfide bonds give exchange reactions between two adjacent S−S bonds via free radicals or ionic intermediates.[17,18] These reactions are activated using photolysis, heating, or oxidation under energies around 210−270 kJ/mol, triggering a decrease of the viscosity that permits the polymer to gain a high molecular mobility state and flow to recover from any distortion, i.e., self-healing.[19] Therefore, since this disulfide exchange can be activated at relatively moderate temperatures, it has attracted the interest of many researchers.[20−23]

Furthermore, this thermal activation may be achieved in different ways. In this regard, the addition of carbon nanostructures promotes resistive heating under Joule's effect. The basis lies in the fact that, due to the electrical networks created by these conductive nanoparticles,[24,25] when applying an electric field, there is a heat dissipation which follows this formula

$$Q = I^2 \cdot R \cdot t \quad (1)$$

where Q is the heat flow, I and R are the current through the material and the electrical resistance, respectively, and t is the time the voltage is applied.

The self-healing activation has been studied in different systems, such as polycaprolactone (PCL)/epoxy[26] and poly-(ethylene-*co*-methacrylic acid) (EMAA) blends[27] or Diels−Alder-based polymer (DAP) dynamic networks,[28] which show a high efficiency with the advantage of low power consumption and the possibility of localized heating.

From the considerations outlined above, this research shifts toward the design of self-healing materials based on disulfide exchange reactions, with the purpose of reaching a material which combines high performance (thermoset behavior) with the ability to recover the original properties of the material under induced damages (thermoplastic behavior). More specifically, the resin will be composed of Bisphenol A diglycidyl ether (DGEBA) functionalized by 2-Aminophenyl disulfide (AFD) hardener in different proportions (stoichiometric; R = 1.0, and with an AFD excess; R = 1.05, R = 1.1). The self-healing efficiency will be studied under convective heating in a conventional oven and under resistive heating when carbon nanotubes (CNTs) are added to the network. The effect of both AFD excess and CNT addition on the thermomechanical and self-healing properties will be studied, and the advantages of conventional or resistive heating will be highlighted.

2. EXPERIMENTAL SECTION

2.1. Materials. Epoxy resin was composed of Bisphenol A diglycidyl ether (DGEBA) functionalized by 2-Aminophenyl disulfide (AFD) hardener in different proportions: stoichiometric; R = 1.0, and with an AFD excess; R = 1.05, R = 1.1, that is, with 5, and 10% of the AFD excess over the stochiometric proportion. They were supplied by Sigma-Aldrich and Tokyo Chemical Industry, respectively.

Multiwalled carbon nanotubes (MWCNTs) used in this study were *NC7000*, supplied by *Nanocyl*. They present an average length of 1.5 μm and an outer diameter of 9.5 nm.

2.2. Manufacturing of 2-AFD/Epoxy Systems. Manufacturing of 2-AFD/epoxy systems was carried out in two different ways, depending on the addition of CNTs.

Neat AFD/epoxy systems were prepared following a modified version of the manufacturing provided by Martinez-Diaz et al.[29] First, the DGEBA monomer is degassed for 15 min at 80 °C instead of heating at 120 °C in order to avoid unwanted side reactions promoted by high temperatures, which could lead to premature curing of the resin. Then, the 2-AFD was added in a stoichiometric proportion of 100:36.5 (DGEBA/AFD; R = 1.0) and with 2-AFD excess (R = 1.05 and R = 1.1), maintaining a temperature of 80 °C. The mixture was magnetically stirred for 5 min for better homogenization. Finally, it was poured into a metallic mold and cured at 160 °C for 6 h.[29]

In the case of CNT-doped AFD/epoxy systems, a previous step was included: the dispersion of the CNTs. It was carried out by means of three-roll milling in an *EXAKT 80E* mini calendar from *EXAKT Technologies Inc.* It consisted of a progressive reduction of the gap between adjacent rolls that rotated in the opposite way. The parameters were set, as shown in Table S1, and are based on previous studies.[30] Then, the mixture was degassed at 80 °C for 15 min, and the AFD was added prior to pouring into the mold and

https://doi.org/10.1021/acsapm.3c01022
ACS Appl. Polym. Mater. 2024, 6, 1106−1115

curing at 160 °C for 6 h, in a similar way to the case of neat AFD/epoxy systems.

2.3. Thermomechanical and Electrical Characterization. Thermomechanical properties were obtained by DMTA, following ASTM 5418, in a *Q800 DMA* device supplied by *TA Instruments*. The tests were carried out in the single cantilever mode with specimens of 35 × 12.7 × 1.7 mm^3 (two per condition). They were subjected to a ramp of 2 °C/min from room temperature to 200 °C.

Furthermore, the electrical properties of CNT-doped samples were determined by means of electrical conductivity measurements. They were conducted according to ASTM D257, using a source measurement unit from *Keithley Instrument Inc.* (mod 2410). Four specimens of 10 × 10 × 1 mm^3 were tested for each condition. The electrical resistance was determined as the slope of the $I-V$ curves with an applied voltage ranging from 0 to 20 and 0−100 V for samples with high and low conductivity, respectively.

Electrothermal properties under resistive heating were also measured. In this case, the voltage was applied in steps of 25 V by using a *Keithley Instrument Inc.* (mod 2410) device. Simultaneously, the temperature was monitored using a thermal camera, *FLIR E50*. A schematic of this test is shown in Figure 1. The electrodes were made of copper wire and sealed with silver ink for proper electrical continuity.

2.4. Self-Healing Tests. The self-healing capabilities of the AFD/epoxy systems were evaluated under different heating sources. First, cracks were induced by using a blade with a cutting edge that formed a 45° edge in the center of the sample.

Once cracks were created, their topology was characterized by means of optical profilometry using a *ZETA Z-20* optical profilometer from *Zeta Inc. Instruments*. For each crack, ten measurements were carried out by taking photograms of 900 × 1000 μm.

After crack characterization, the samples were subjected to a thermal stimulus in order to reach the necessary temperature to activate the healing mechanisms. This thermal activation was carried out by means of convective heating in a conventional oven in the case of neat AFD/epoxy systems and by convective and resistive heating in the case of CNT-doped ones.

The repaired cracks were characterized by optical profilometry, and the mechanical properties were assessed via three-point bending testing. The healing efficiency, η, was defined as follows

$$\eta(\%) = \frac{X_f}{X_0} \times 100 \tag{2}$$

where X_0 and X_f were the initial and after-healing volume of the crack from the optical profilometry characterization, respectively, and the nominal (nondamaged virgin sample) and after-healing flexural strengths, respectively.

The initial and after-healing volumes were calculated and characterized from the images taken by the profilometer by using the analysis software *MountainsMap*.

The nominal and after-healing flexural strengths were calculated and characterized from the three-point bending test carried out in a Zwick Z100 (Zwick-Roell, Ulm, Germany) universal tensile machine according to the standard ASTM D790. The bending force was applied on top of the healed crack, in the case of the healed samples, and the tests were conducted at 10.05 mm/min up to failure to obtain the flexural strength.

3. RESULTS AND DISCUSSION

In this section, an analysis of the self-healing efficiency of the 2-AFD/epoxy system using different heating sources is presented. First, the effect of the monomer-to-hardener ratio on the thermomechanical properties is explored, and the most relevant self-healing results from convection heating in a conventional oven are discussed. Then, the effect of CNT addition on the electrical and thermomechanical properties is investigated, and the self-healing results under Joule's heating are shown and compared to conventional convection heating.

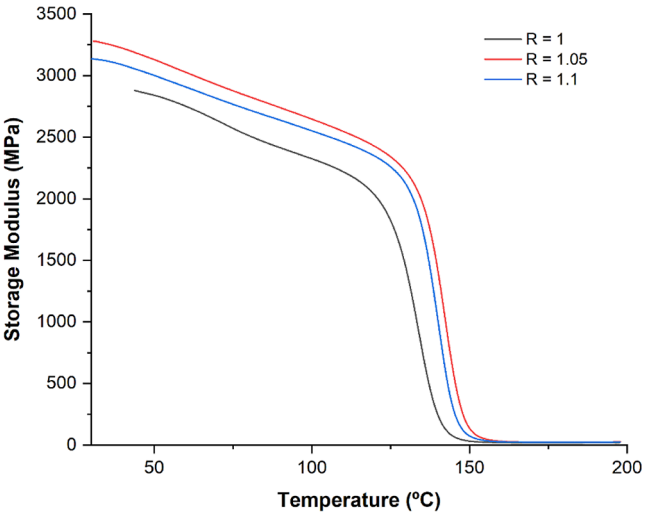

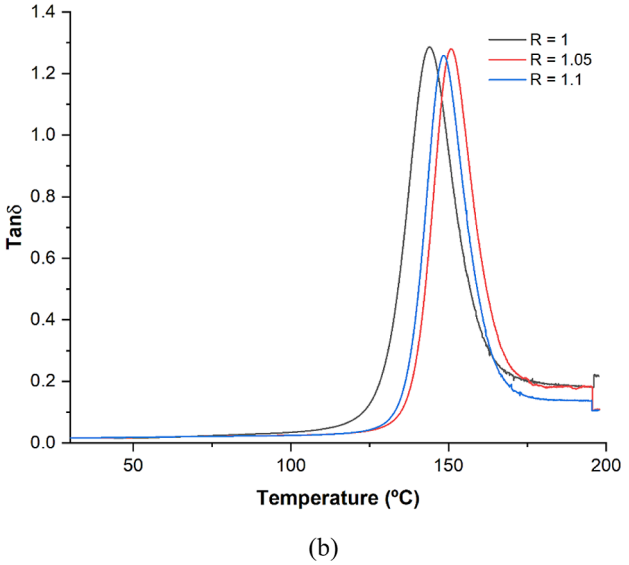

Figure 2. Results of DMTA tests showing (a) storage modulus and (b) tan δ as a function of temperature.

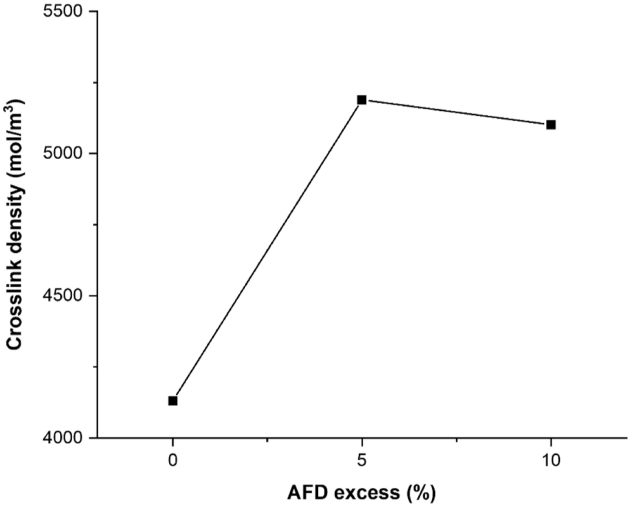

Figure 3. Cross-link density as a function of AFD excess.

https://doi.org/10.1021/acsapm.3c01022
ACS Appl. Polym. Mater. 2024, 6, 1106−1115

Table 1. Values of the Self-Healing Efficiency for Different AFD/Epoxy Proportions

condition	efficiency (%)
R = 1.0	94 ± 2
R = 1.05	97 ± 2
R = 1.1	97 ± 1

3.1. Analysis of the Neat 2-AFD/epoxy System.

3.1.1. Thermomechanical Properties. Figure 2 shows the results of the DMTA tests for the different hardener-to-monomer ratios. Here, several facts can be observed.

On the one hand, there is an increase of the storage modulus (E′) with increasing AFD content (Figure 2a), since the

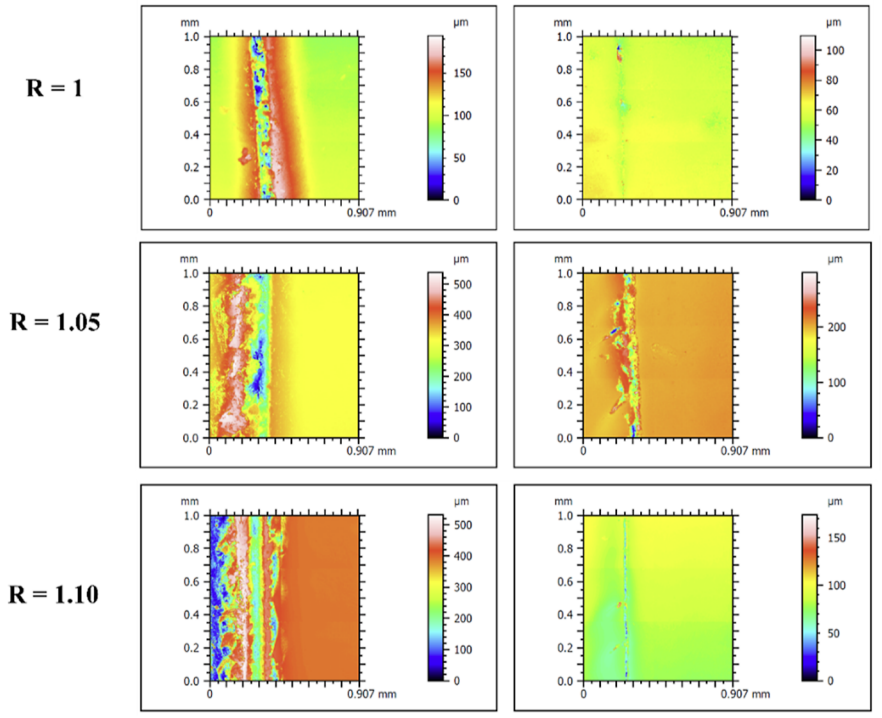

(a)

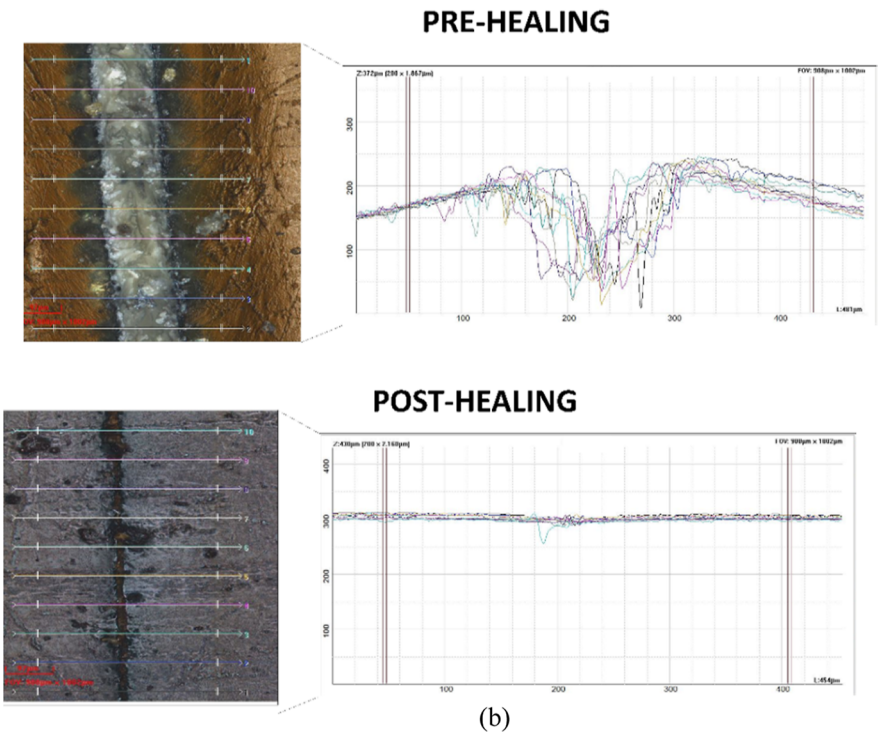

(b)

Figure 4. (a) Map contour of the crack before (left) and after (right) the healing process for different conditions and (b) profile contour of the crack before and after the healing process.

https://doi.org/10.1021/acsapm.3c01022
ACS Appl. Polym. Mater. 2024, 6, 1106−1115

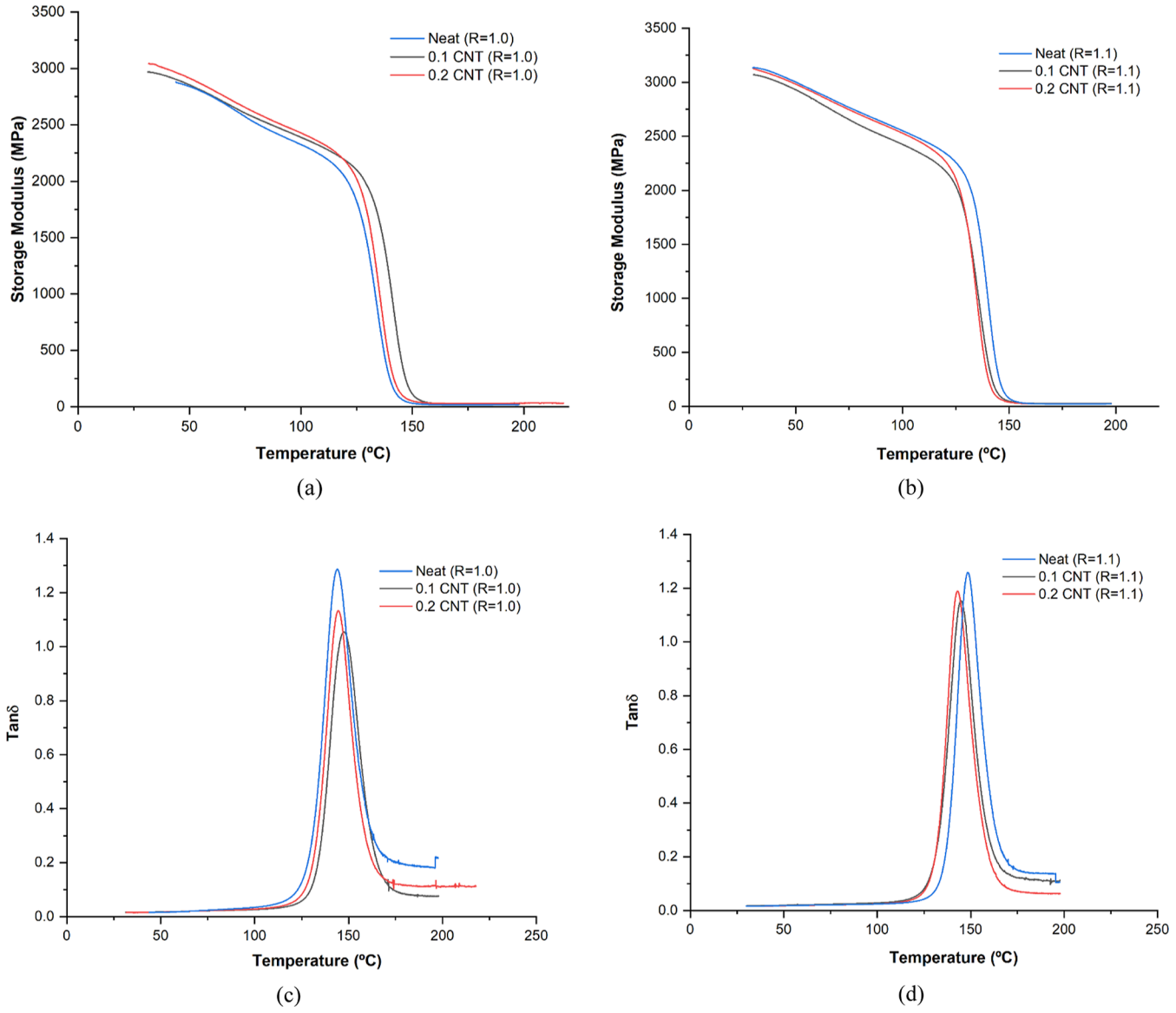

Figure 5. DMTA results showing the storage modulus as a function of temperature for (a) R = 1.0 and (b) R = 1.1 and the values of tan δ for (c) R = 1.0 and (d) R = 1.1.

stoichiometric network has most of the amine-epoxi bonds formed but is a less packed and more open network.[31] When there is an excess of AFD, the addition of amines eases the reaction between amines and epoxy groups, increasing the number of reacted molecules and achieving a higher chemical conversion.

In order to better understand the effect of chain mobility on the thermomechanical properties of the system, it is possible to estimate the cross-link density according to the following formula[32]

$$\upsilon_c = \frac{E'}{3RT} \tag{3}$$

where E' is the storage modulus in the rubbery region (at T_g + 30 K), R in the universal gas constant, and T is equal to T_g + 30 K.

In this regard, Figure 3 shows the calculated values of cross-link density for different conditions. It can be observed that, by increasing the AFD content, the cross-linking density increases. This would also be in good agreement with the observed increment in the storage modulus at room temperature since the increase of reacted amine/epoxy groups leads to networks with a higher number of cross-linking points.

On the other hand, the evolution of the ratio E″/E′ (being E′ and E″ the storage and loss moduli, respectively), that is, tan δ for each condition, is shown in Figure 2b. Here, two important facts can be stated: on the one hand, the maximum temperature of the tan δ peak increases with the AFD content. This fact means that the T_g, estimated as the peak of tan δ, that is, when the correlation between the viscoelastic and elastic behavior of the polymer is maximum, increases with the AFD content, as observed in Table S2. This is in good agreement with the previously commented increase of the cross-linking degree. Therefore, the presence of an excess of amines is reflected in an increase of the thermomechanical properties, both in terms of storage modulus as well as concerning the value of T_g.

Furthermore, it can also be stated that the width of the tan δ peak is quite similar in every case, which is indicative of a homogeneous polymer network.

https://doi.org/10.1021/acsapm.3c01022
ACS Appl. Polym. Mater. 2024, 6, 1106−1115

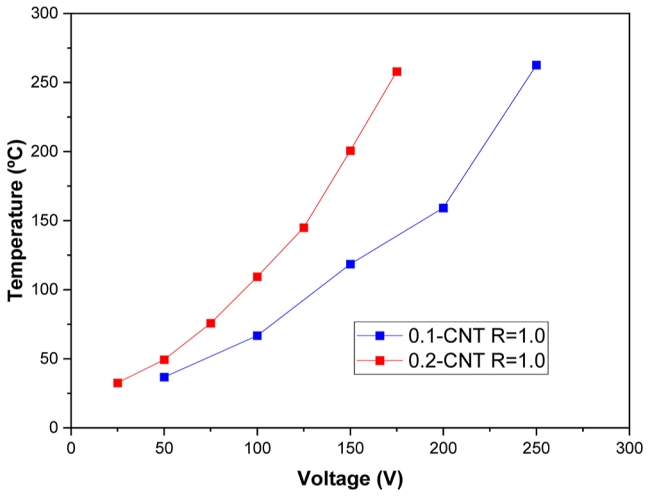

(a)

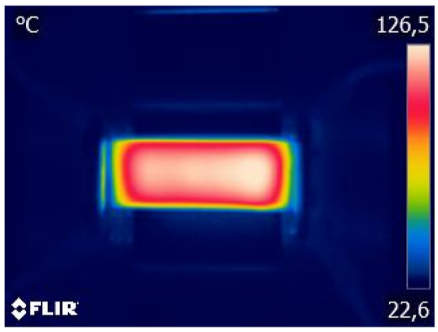

(b)

Figure 6. Results of the resistive heating showing (a) temperature-voltage curves and (b) image of the thermal camera showing the homogeneity of heating.

Table 2. Values of Self-Healing Efficiency for the Different AFD/Epoxy Nanocomposites under Convection (conv) and Resistive (Joule) Heating

condition	efficiency conv. (%)	efficiency Joule (%)
neat R = 1.0	94.07 ± 1.55	N/A
0.1 CNT R = 1.0	99.21 ± 1.09	95.96 ± 1.67
0.2 CNT R = 1.0	94.52 ± 1.56	98.22 ± 1.09

3.1.2. Self-Healing Efficiency. Table 1 summarizes the self-healing efficiencies of neat 2-AFD systems under conventional heating in a convection oven. In every case, the temperature was set as $T_{g\text{-min}}$ + 80 °C, where $T_{g\text{-min}}$ was set as the minimum glass transition temperature of all of the systems. Moreover, the healing time was set at 1.5 h to guarantee that the self-healing mechanisms took place.

It can be observed that the healing efficiencies were above 94% in every case. This is indicative that the healing process is taking place in an efficient way, with an almost total recovery of the induced crack. By deeply analyzing the results, it can be elucidated that, by increasing the AFD content, the healing efficiency increases due to the presence of a polymer network with higher mobility, which facilitates the healing process. However, the differences observed are very slight, almost overshadowed by standard deviations.

The efficiency of the self-healing process is highlighted in Figure 4, where the images of the crack before and after the convective healing process are shown. In every case, an almost total recovery of the crack is observed (Figure 4a). The same effect is observed when analyzing the profile contours, where a practically flat surface is observed after the healing process (Figure 4b).

Here, it is important to point out that the healing efficiencies reached in every case are significantly above those obtained for similar systems based on epoxy/PCL blends.[26,33] This could be explained because of the discrete distribution of the thermoplastic phase in these systems, which could affect the healing process, promoting an irregular recovery throughout the crack.

3.2. Analysis of the CNT-Doped 2-AFD/epoxy System.

3.2.1. Thermomechanical Properties. After observing a similar self-healing behavior regardless of the AFD excess on the system, the effect of CNT addition will be studied only for the systems with R = 1 and R = 1.1. The reason lies in the fact that the stoichiometric condition proved enough healing efficiency and a reduced T_g, which leads to lower self-healing temperatures. In addition, an excess of AFD could promote early degradation of the material. On the other hand, the R = 1.1 system is selected due to the increase of thermomechanical properties provided by an excess of AFD, as observed before. Although the R = 1.05 system shows a slight increment of the storage modulus in comparison with the R = 1.1 system, this study aims to understand the role of the AFD excess in the CNT-polymer network so that a higher content of AFD excess may be more relevant for this purpose.

In this regard, Figure 5 and Table S3 summarize the thermomechanical behavior determined by the DMTA analysis of the different samples. Here, several facts can be stated.

On the one hand, the storage modulus at room conditions slightly increases with the CNT addition (Figure 5a,b). However, there are some differences between the behavior of R = 1.0 and R = 1.1 samples. In the stoichiometric condition, the increase of storage modulus is prevalent at higher CNT contents (0.2 wt %). This can be explained by the stiffening effect of the CNTs themselves, and it is indicative of their good distribution. In the case of R = 1.1, there is not a significant variation of E′ other than a slight decrease in the vitreous region. This effect can be explained by the presence of some unreacted domains. In this case, these unreacted domains could lead to a saturation of the network, with the presence of larger aggregates that may induce a weakening effect in the network, and thus, the addition of CNTs may not promote the same stiffening effect as the one observed with the stoichiometric content.

On the other hand, Figure 5c,d shows the tan δ curves for the different CNT conditions. Here, it can be observed that the width of the tan δ peaks is quite similar in every case, with no presence of another peak, indicating that the CNTs do not promote heterogeneities in the network in comparison to the neat resin conditions. When observing the maximum value of tan δ peaks, it can be observed that, for R = 1.0, this value decreases with the incorporation of CNTs but maintains similar values between the 0.1 and 0.2 wt % CNTs systems.

This is indicative of the dissipative energy of the system. A higher value of tan δ implies a higher dissipation energy of the system and, thus, more prevalent viscoelastic behavior. As explained before, the stiffening effect of the CNTs leads to an increase of E′ and, consequently, a reduction of the tan δ value, as observed in the stoichiometric conditions. However, when adding an AFD excess (R = 1.1), the unreacted domains lead to a saturation of the network so that the global network is not

https://doi.org/10.1021/acsapm.3c01022
ACS Appl. Polym. Mater. 2024, 6, 1106−1115

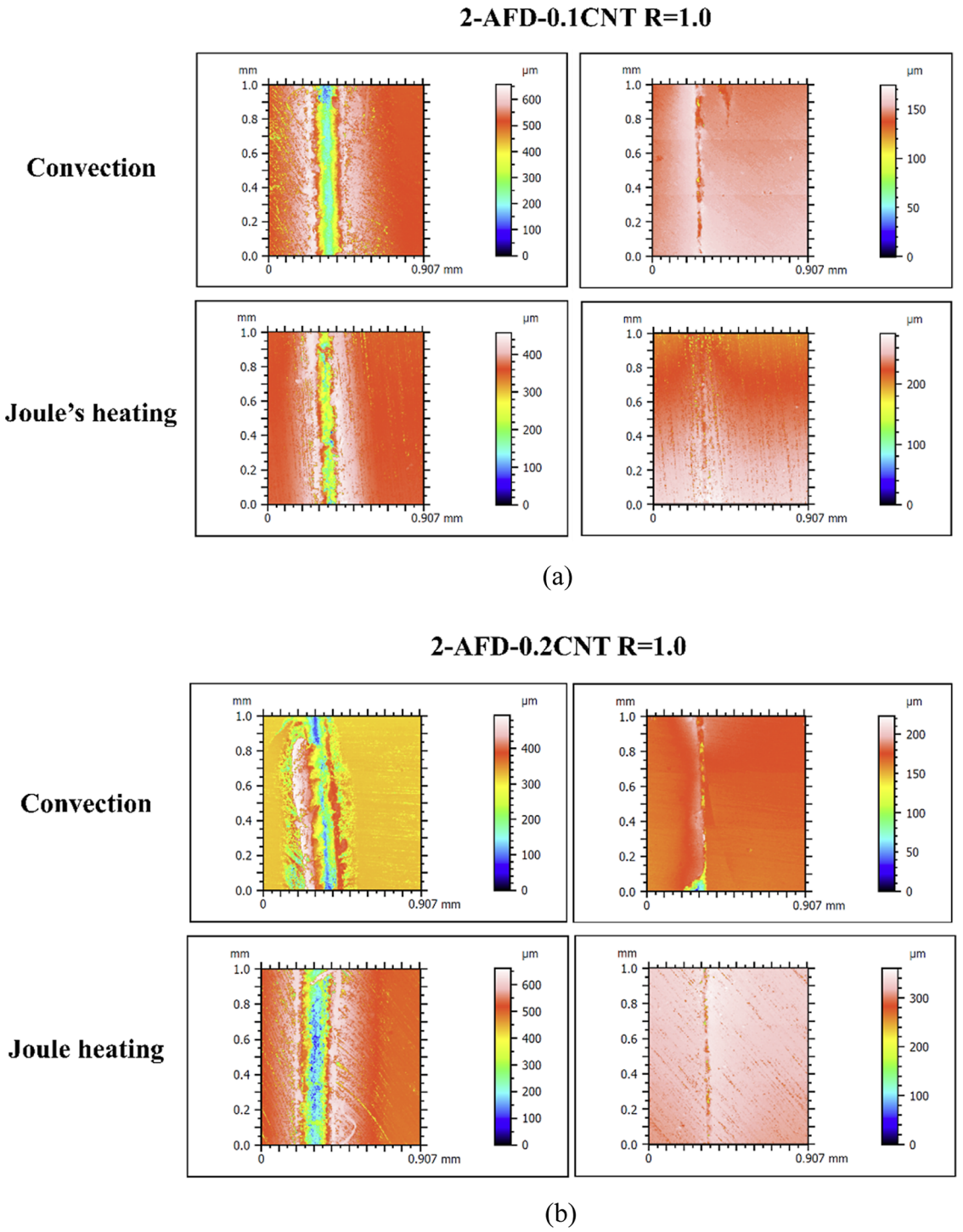

Figure 7. Map contours before (left) and after (right) the healing process for (a) 0.1 and (b) 0.2 CNT samples under convection and resistive heating.

severely affected, as observed before in the storage modulus behavior.

3.2.2. Electrical and Electrothermal Properties. The electrical properties of CNT samples are analyzed in order to understand their resistive heating capabilities. In this context, Table S4 shows the values of the electrical conductivity under the different CNT conditions.

Here, two effects can be observed. On the one hand, the electrical conductivity increases with CNT content, as expected, due to the higher number of electrical pathways. On the other hand, when increasing the AFD content, a reduction in the electrical conductivity is observed, playing a very prevalent role in the electrical properties of the material.

This drastic reduction of the electrical conductivity from R = 1.0 to R = 1.1 (around an order of magnitude) can be explained because of the efficiency of the electrical network. As commented before, when increasing the AFD content above the stoichiometric proportion, the presence of some unreacted domains may promote a higher CNT aggregation, and, thus,

https://doi.org/10.1021/acsapm.3c01022
ACS Appl. Polym. Mater. 2024, 6, 1106−1115

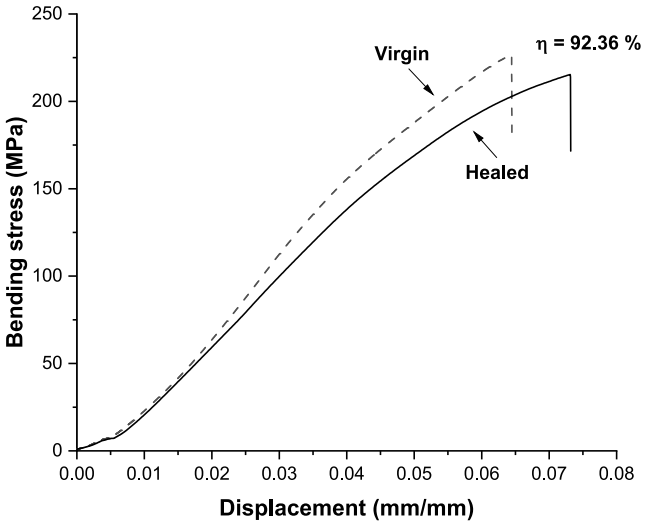

Figure 8. Representative stress−strain curves for a virgin (nondamaged) sample and a healed sample of the 2-AFD-0.2CNT (R = 1.0) system.

this is reflected in a much less efficient network,[34,35] leading to a drastic reduction of the electrical conductivity.

Furthermore, the electrical conductivity values of the R = 1.0, especially at 0.1 wt % CNT, are much higher than those observed in other similar systems,[34,36] indicating that the distribution of the CNTs is quite optimal, and thus, the electrical network is the most efficient. For this reason, Joule's heating capabilities were studied for the R = 1.0 samples, as the resistive heating capabilities are directly correlated to the electrical conductivity, and these samples showed the best electrical properties.

In this regard, Figure 6 shows the resistive heating behavior of R = 1.0, 0.1, and 0.2 CNT samples. Here, it can be observed that the temperature reached in the sample increases following a quadratic law with the voltage applied (Figure 6a), as expected due to the correlation between the heat flow and the voltage−current according to Joule's law (eq 1). In addition, the samples with 0.2 wt % CNT presented the highest resistive heating capabilities, as expected due to their higher electrical conductivity. More specifically, the voltage needed to reach $T_{g\text{-min}}$ + 80 °C was 220 and 150 V for 0.1 and 0.2 wt % CNT, respectively. Furthermore, the analysis of the IR images showed homogeneous heating around the sample (Figure 6b), which is explained by the homogeneous CNT distribution.

3.2.3. Self-Healing Analysis. In the case of CNT-doped samples, as commented before, the self-healing efficiency has been analyzed by convection heating in a conventional oven (such as in the case of neat samples) and by resistive heating. Here, only the stoichiometric samples were studied as they showed very high healing efficiencies in the neat systems, and the electrothermal properties under resistive heating were found to be the best in the case of CNT-doped ones.

In this regard, Table 2 summarizes the self-healing efficiencies achieved by these two methods. Here, several facts can be stated.

On the one hand, it can be observed that, in every case, the healing efficiency is far above 90%, indicating a practically total recovery of the crack during the healing process. More specifically, it can be observed that the CNT addition does not negatively affect the healing efficiency, as the CNTs do not interfere with the chain mobility during the healing process. It is also an indicator of good homogeneity of the network, facilitated by good CNT dispersion, as previously explained.

On the other side, it can be elucidated that the healing efficiencies of both convective and resistive heating were found to be very similar. Here, the good CNT distribution promotes homogeneous resistive heating, as shown before, and thus, there is homogeneous chain mobility during the healing process. In fact, the images of pre- and posthealing are shown in Figure 7, indicating that the recovery of the crack both after convective and resistive heating is practically total, so the crack is completely closed.

The mechanical testing carried out on the 2-AFD-0.2CNT (R = 1.0) samples confirmed the efficiency of the healing process. Here, the 0.2 wt % CNT content was selected as it would be the most critical condition to evaluate the mechanical performance due to the higher CNT entanglement. As shown in Figure 8, the stress−strain curve of the healed samples closely matched that of the nondamaged sample, showing a mechanical self-healing efficiency of 92.36% after being damaged and subsequently healed via resistive heating, thus recovering most of the nondamaged mechanical properties. Therefore, these results corroborate those obtained from the optical profilometer, which showed similar healing efficiencies of above 90%.

Therefore, the analysis of the self-healing process highlights the potential of resistive heating, as it is possible to achieve very similar healing efficiencies as convective heating but with much lower power consumption and the possibility of local heating in the damaged zone.

4. CONCLUSIONS

The self-healing capabilities of 2-AFD/epoxy systems were explored by using convective and resistive heating as thermal stimuli.

The thermomechanical analysis of neat 2-AFD/epoxy systems with different AFD to DGEBA ratios showed that an increase of 2-AFD excess leads to an increase in both the storage modulus and the T_g. This can be explained by an increment of the cross-link density with increasing the AFD content, calculated from the storage modulus in the rubbery region due to the presence of more amine molecules, which facilitates the reaction between amines and epoxy groups.

The analysis of the self-healing capabilities of an induced crack showed a similar healing efficiency for every AFD content, with values above 90% in every case, highlighting the huge potential of these systems for healing purposes. For these reasons and due to the superior thermomechanical properties, only the stoichiometric and R = 1.1 conditions were analyzed when adding CNTs.

CNT affects the thermomechanical properties of the AFD system under stoichiometric conditions. More specifically, an increase of the storage modulus at room temperature was observed, whereas T_g was not severely affected. The first effect was mainly associated with the stiffening effect of the CNTs. Here, the presence of excess AFD (R = 1.1) does not reflect any effect on the thermomechanical properties, as the unreacted molecules may promote a higher CNT entanglement. This is reflected in a reduction of the electrical conductivity and lower resistive heating capabilities in comparison to the stoichiometric conditions (R = 1.0). That is why the self-healing efficiencies were only explored for the CNT-doped stoichiometric system.

https://doi.org/10.1021/acsapm.3c01022
ACS Appl. Polym. Mater. 2024, 6, 1106−1115

The analysis of the self-healing capabilities of CNT-doped samples showed very high healing efficiencies (above 90%) in every condition, both by convective and by resistive heating. Here, the main advantage of resistive heating over convective heating was found to be the lower power consumption and the possibility of localized heating.

Therefore, the addition of CNT to AFD/epoxy systems opens a way for self-healing activation under resistive heating without any detriment to the healing efficiency of these systems.

■ ASSOCIATED CONTENT

Data Availability Statement

The raw/processed data required to reproduce these findings cannot be shared at this time due to technical or time limitations.

Supporting Information

The Supporting Information is available free of charge at https://pubs.acs.org/doi/10.1021/acsapm.3c01022.

Additional details of the experimental setup and glass transition temperature and electrical conductivity results for all compounds (PDF)

■ AUTHOR INFORMATION

Corresponding Author

Xoan Xosé Fernández Sánchez-Romate − *Materials Science and Engineering Area, Escuela Superior de Ciencias Experimentales y Tecnología, Universidad Rey Juan Carlos, 28933 Móstoles, Madrid, Spain;* orcid.org/0000-0001-9283-4712; Email: xoan.fernandez.sanchezromate@urjc.es

Authors

Javier Gómez-Sánchez − *Materials Science and Engineering Area, Escuela Superior de Ciencias Experimentales y Tecnología, Universidad Rey Juan Carlos, 28933 Móstoles, Madrid, Spain*

Alberto Jiménez-Suárez − *Materials Science and Engineering Area, Escuela Superior de Ciencias Experimentales y Tecnología, Universidad Rey Juan Carlos, 28933 Móstoles, Madrid, Spain;* orcid.org/0000-0001-8416-6398

Silvia G. Prolongo − *Materials Science and Engineering Area, Escuela Superior de Ciencias Experimentales y Tecnología, Universidad Rey Juan Carlos, 28933 Móstoles, Madrid, Spain;* orcid.org/0000-0002-4438-6123

Complete contact information is available at: https://pubs.acs.org/10.1021/acsapm.3c01022

Notes

The authors declare no competing financial interest.

■ ACKNOWLEDGMENTS

This work was supported by the Agencia Estatal de Investigación of the Spanish Government [PROJECT PID2019-106703RB-I00]; the Young Researchers R&D Project [ref. M2183, SMART-MULTICOAT] funded by Universidad Rey Juan Carlos and Comunidad de Madrid; and the PREDOC PhD funding program of the Universidad Rey Juan Carlos.

■ REFERENCES

(1) Gauthier, M. M. *Engineered Materials Handbook*; ASM International, 1995; pp 1−1300.

(2) Li, W.; Xiao, L.; Wang, Y.; Chen, J.; Nie, X. Self-healing silicon-containing eugenol-based epoxy resin based on disulfide bond exchange: Synthesis and structure-property relationships. *Polymer* **2021**, *229*, 123967.

(3) Barile, M.; Lecce, L.; Iannone, M.; Pappadà, S.; Roberti, P. *Thermoplastic Composites for Aerospace Applications*; Revolutionizing aircraft materials and processes; Springer, 2020; pp 87−114.

(4) Postiglione, G.; Turri, S.; Levi, M. Effect of the plasticizer on the self-healing properties of a polymer coating based on the thermoreversible Diels-Alder reaction. *Prog. Org. Coat.* **2015**, *78*, 526−531.

(5) Urdl, K.; Kandelbauer, A.; Kern, W.; Müller, U.; Thebault, M.; Zikulnig-Rusch, E. Self-healing of densely crosslinked thermoset polymers—a critical review. *Prog. Org. Coat.* **2017**, *104*, 232−249.

(6) Paolillo, S.; Bose, R. K.; Santana, M. H.; Grande, A. M. Intrinsic self-healing epoxies in polymer matrix composites (PMCs) for aerospace applications. *Polymers* **2021**, *13*, 201.

(7) Kishi, H.; Nakamura, T.; Hagiwara, S.; Urahama, Y. Thermo-reversible phase structures of lightly cross-linked PDMS/MQ silicone polymer blends. *Polymer* **2020**, *200*, 122574.

(8) Rahmatpour, A.; Alijani, N.; Mirkani, A. Supramolecular self-assembling hydrogel film based on a polymer blend of chitosan/partially hydrolyzed polyacrylamide for removing cationic dye from water. *React. Funct. Polym.* **2023**, *185*, 105537.

(9) Blaiszik, B. J.; Kramer, S. L.; Olugebefola, S. C.; Moore, J. S.; Sottos, N. R.; White, S. R. Self-healing polymers and composites. *Annu. Rev. Mater. Res.* **2010**, *40*, 179−211.

(10) O'Donnell, A. D.; Salimi, S.; Hart, L. R.; Babra, T. S.; Greenland, B. W.; Hayes, W. Applications of supramolecular polymer networks. *React. Funct. Polym.* **2022**, *172*, 105209.

(11) van Gemert, G. M.; Peeters, J. W.; Söntjens, S. H. M.; Janssen, H. M.; Bosman, A. W. Self-healing supramolecular polymers in action. *Macromol. Chem. Phys.* **2012**, *213*, 234−242.

(12) Kalista, S. J., Jr; Ward, T. C. Thermal characteristics of the self-healing response in poly (ethylene-co-methacrylic acid) copolymers. *J. R. Soc. Interface* **2007**, *4*, 405−411.

(13) Mo, J.; Chen, X.; Fu, Y.; Li, R.; Lin, Y.; Zhang, A. A solvent-free, transparent, self-healing polysiloxanes elastomer based on unsaturated carboxyl-amino ionic hydrogen bonds. *Polymer* **2021**, *228*, 123903.

(14) Peng, Y.; Yang, Y.; Wu, Q.; Wang, S.; Huang, G.; Wu, J. Strong and tough self-healing elastomers enabled by dual reversible networks formed by ionic interactions and dynamic covalent bonds. *Polymer* **2018**, *157*, 172−179.

(15) Burattini, S.; Greenland, B. W.; Merino, D. H.; Weng, W.; Seppala, J.; Colquhoun, H. M.; Hayes, W.; Mackay, M. E.; Hamley, I. W.; Rowan, S. J. A healable supramolecular polymer blend based on aromatic π- π stacking and hydrogen-bonding interactions. *J. Am. Chem. Soc.* **2010**, *132*, 12051−12058.

(16) Benazzo, F.; Sodano, H. A. Evaluation of Interfacial Shear Strength Healing Efficiency between Dynamic Covalent Bond-Based Epoxy and Functionalized Fiberglass. *ACS Appl. Polym. Mater.* **2022**, *4*, 2925−2934.

(17) Islam, S.; Bhat, G. Progress and challenges in self-healing composite materials. *Mater. Adv.* **2021**, *2*, 1896−1926.

(18) Zhou, Q.; Zhu, X.; Zhang, W.; Song, N.; Ni, L. Recyclable High Performance Epoxy Composites Based on Double Dynamic Carbon-Nitrogen and Disulfide Bonds. *ACS Appl. Polym. Mater.* **2020**, *2*, 1865−1873.

(19) Takahashi, A.; Ohishi, T.; Goseki, R.; Otsuka, H. Degradable epoxy resins prepared from diepoxide monomer with dynamic covalent disulfide linkage. *Polymer* **2016**, *82*, 319−326.

(20) Zheng, X.; Yang, H.; Sun, Y.; Zhang, Y.; Guo, Y. A molecular dynamics simulation on self-healing behavior based on disulfide bond exchange reactions. *Polymer* **2021**, *212*, 123111.

(21) Xiang, H.; Yin, J.; Lin, G.; Liu, X.; Rong, M.; Zhang, M. Photo-crosslinkable, self-healable and reprocessable rubbers. *Chem. Eng. J.* **2019**, *358*, 878−890.

(22) Tran, V. T.; Mredha, M. T. I.; Na, J. Y.; Seon, J.; Cui, J.; Jeon, I. Multifunctional poly(disulfide) hydrogels with extremely fast self-healing ability and degradability. *Chem. Eng. J.* **2020**, *394*, 124941.
(23) Ozawa, M.; Shibata, M. Reprocessable bismaleimide-diamine thermosets based on disulfide bonds. *React. Funct. Polym.* **2020**, *146*, 104404.
(24) Zhi, X.; Liu, J.; Zhang, H.; Hong, S.; Yu, Z. Simultaneous enhancements in electrical conductivity and toughness of selectively foamed polycarbonate/polystyrene/carbon nanotube microcellular foams. *Composites, Part B* **2018**, *143*, 161−167.
(25) Song, Y. S.; Youn, J. R. Influence of dispersion states of carbon nanotubes on physical properties of epoxy nanocomposites. *Carbon* **2005**, *43*, 1378−1385.
(26) Sánchez-Romate, X. F.; Sans, A.; Jiménez-Suárez, A.; Prolongo, S. G. The addition of graphene nanoplatelets into epoxy/polycaprolactone composites for autonomous self-healing activation by Joule's heating effect. *Compos. Sci. Technol.* **2021**, *213*, 108950.
(27) Wang, W.; Ouyang, Q.; Liu, L.; Wu, Z. Novel nanotube/poly(ethylene-co-methacrylic acid)/epoxy composite adhesive possessing in-situ electrical-heating activated crack healing function. *Compos. Part A Appl. Sci. Manuf.* **2021**, *150*, 106599.
(28) Sang, Z.; Zhou, Q.; Kumar Rajagopalan, K.; Thomas, E. L.; Gardea, F.; Sukhishvili, S. A. Dynamic polymer network conductive Nanocomposites: Low percolation threshold and Joule-heating-induced network plasticity. *Chem. Eng. J.* **2022**, *443*, 136400.
(29) Martinez-Diaz, D.; Cortés, A.; Jiménez-Suárez, A.; Prolongo, S. G. Hardener Isomerism and Content of Dynamic Disulfide Bond Effect on Chemical Recycling of Epoxy Networks. *ACS Appl. Polym. Mater.* **2022**, *4*, 5068−5076.
(30) Sánchez-Romate, X. F.; Jiménez-Suárez, A.; Sánchez, M.; Güemes, A.; Ureña, A. Novel approach to percolation threshold on electrical conductivity of carbon nanotube reinforced nanocomposites. *RSC Adv.* **2016**, *6*, 43418−43428.
(31) Aguirre De Cárcer, I.; González Prolongo, M.; Salom Coll, C.; Parrado, J.; Moriche, R.; González Prolongo, S. Thermal and mechanical properties of self-healing epoxy/graphene nanocomposites. In *VIII ECCOMAS Thematic Conference on Smart Structures and Materials SMART*, 2017;.
(32) Hill, L. W. Calculation of crosslink density in short chain networks. *Prog. Org. Coat.* **1997**, *31*, 235−243.
(33) Jiménez-Suárez, A.; Del Rosario, G.; Sánchez-Romate, X. X.; Prolongo, S. G. Influence of Morphology on the Healing Mechanism of PCL/Epoxy Blends. *Materials* **2020**, *13*, 1941.
(34) Sánchez-Romate, X. F.; Artigas, J.; Jiménez-Suárez, A.; Sánchez, M.; Güemes, A.; Ureña, A. Critical parameters of carbon nanotube reinforced composites for structural health monitoring applications: Empirical results versus theoretical predictions. *Compos. Sci. Technol.* **2019**, *171*, 44−53.
(35) Li, J.; Ma, P. C.; Chow, W. S.; To, C. K.; Tang, B. Z.; Kim, J. Correlations between percolation threshold, dispersion state, and aspect ratio of carbon nanotubes. *Adv. Funct. Mater.* **2007**, *17*, 3207−3215.
(36) Mousavi, S. R.; Estaji, S.; Kiaei, H.; Mansourian-Tabaei, M.; Nouranian, S.; Jafari, S. H.; Ruckdäschel, H.; Arjmand, M.; Khonakdar, H. A. A review of electrical and thermal conductivities of epoxy resin systems reinforced with carbon nanotubes and graphene-based nanoparticles. *Polym. Test.* **2022**, *112*, 107645.

https://doi.org/10.1021/acsapm.3c01022
ACS Appl. Polym. Mater. 2024, 6, 1106−1115